HEAD IMPACTS AND BRAIN INJURY IN FATALLY INJURED PEDESTRIANS

GA RYAN*, AJ McLEAN*, ATS VILENIUS*, CN KLOEDEN*,
DA SIMPSON* and PC BLUMBERGS+

*NHMRC Road Accident Research Unit,
University of Adelaide, South Australia.

+Division of Tissue Pathology,
Institute of Medical & Veterinary Science,
Adelaide, South Australia.

INTRODUCTION

At-the-scene studies of road traffic accidents have been conducted by the Road Accident Research Unit, and its predecessor, at the University of Adelaide since 1963.[1,2,3] These studies confirmed the importance of impacts to the head, even in an environment of compulsory helmet wearing by motorcyclists and belt use by vehicle occupants.[4,5,6]

Since 1981 the National Health and Medical Research Council has provided relatively long-term support for the work of the Road Accident Research Unit. This has made it feasible for us to conduct a major study of the mechanisms of injury to the brain in actual road crashes. The study, which is described in greater detail later in this paper, involves an attempt to relate the nature and severity of the impact to the head to the nature and severity of the resulting injury to the brain in fatal cases. As such, it complements other approaches to the study of brain injury mechanisms.

Experimental studies have provided the basis of our understanding of the mechanisms of injury to the brain due to blunt impact. They have the great advantage which comes from being able to specify the nature and severity of the impact to the head, or at least measure the resulting acceleration.[7,8] However they also have the limitations inherent in the need to extrapolate from the cadaver, or the animal surrogate, to the living human. Experimental studies using human volunteers, including professional boxers, have no bio-fidelity limitations but they are unlikely to provide information on impacts which cause injury.[9]

Observational studies, of the type reported here, are well-suited to the description of the nature and severity of the injuries to the brain but reconstruction of the nature and severity of the impact is difficult and often of doubtful validity. We now proceed to describe how we have attempted to deal with these difficulties.

METHOD

Pedestrian head impacts were chosen for detailed study because the kinematics of the collision were thought to be relatively uncomplicated; there is often only one impact to the head, and its magnitude can be estimated. This provides a means of investigating the relationship between brain injury patterns and impacts of known magnitude and direction.

Investigative Procedures

The steps in working up a case of fatal injury involving a pedestrian are as follows:

1. All persons dying as a result of a road crash in South Australia are subjected to a post mortem examination. By arrangement with the

Coroner, a member of the Unit staff attends the autopsy of all pedestrian fatalities. At autopsy particular attention is paid to superficial injuries, as they can reveal much about the structures impacted and the position and orientation of the pedestrian relative to the car, and also injuries to the head, scalp and skull. A photographic record is made of all injuries to the body, using colour reversal film.

2. During the examination of the vehicle, measurements are made to locate the position of any damage and deformation, including marks and other signs of contact between the pedestrian and the car. These marks are referred to in determining the pedestrian's orientation to the car at impact. Once again, a photographic record is made of all relevant features of the damage to the vehicle.
3. At the crash site, measurements and photographs are made of all skid marks, gouges, scrapes, blood stains and other markings, as well as the final positions of the body and the vehicle, as indicated by the police Accident Investigation Unit.
4. The sequence of events occurring in the crash is established by reviewing the physical evidence from the autopsy, the vehicle, and the crash site, together with descriptions of the collision given by the driver and any witnesses.
5. The impact velocity of the vehicle is estimated by assessment of all available sources of information, e.g. length of skid marks [10], projection distance of the body [11], vehicle damage, driver and witness statements. In 80% of cases estimates from three or more sources are available for making a final estimate.
6. The stiffness of the panel struck is estimated by reference to the appropriate literature [12], then basic engineering calculations are carried out to establish initial relative static stiffness estimates with respect to tested panels. The stiffness of the head was estimated from reference [13]. Then a combined stiffness, of head and panel together, is estimated.
7. The location of the impact point on the head is determined from superficial markings e.g. abrasions, bruises, and from bruising under the scalp, which may be revealed when the scalp is reflected. The location of the impact is recorded using a system of coordinates, similar to latitude and longitude. There are four equally spaced horizontal zones above, and four below, a line through the top of the external auditory meatus and the lateral canthus of the eye. There are also 12 vertical zones, each of 30°, measured clockwise from the midline anteriorly when viewed from above. Thus, the general position of an impact can be specified by two numbers (Figure 1).
8. After removal at autopsy, the brain is placed in concentrated formalin and transported to the Head Injury Laboratory of the Division of Tissue Pathology at the Institute of Medical and Veterinary Science. Here, after a minimum fixation period of two weeks, the brain is sectioned at 10mm intervals and examined macroscopically. Each section is photographed in black and white. Histological slides of the whole brain sections are prepared and stained using standard neuropathological techniques. These slides are examined microscopically by a neuropathologist (PCB), for signs such as vascular damage, axonal and hypoxic injury. Silver staining techniques supplemented by immunohistochemical methods for neurofilament proteins are used to detect the presence of diffuse axonal injury. Immunohistochemical methods are used to detect the presence of glial fibrillary acidic protein.
9. When lesions are observed they are recorded using line diagrams of the 10 standard coronal cross sections of the cerebral hemispheres which

we have developed for this purpose (Figure 1). Each section is divided into one central and 8 radial sectors. The anterior parts of the temporal lobes are recorded separately. Within each sector the severity of an injury is recorded using an elementary 0, 1, 2, 3 severity scale for cortex and white matter separately. The presence of subdural or subarachnoid haemorrhage is also recorded. The total injury score for each sector in each of the 10 cross sections is coded and entered into a computer file. In this way the distribution as well as the severity of injury throughout a single brain is recorded in three dimensions.

ANALYSIS

Over the past 5 years we have conducted a detailed investigation of 150 pedestrian fatalities. These cases constitute an almost complete sample of pedestrian fatalities occurring in Adelaide. Twenty-six of these cases involved a single pedestrian/vehicle collision in which there was only one impact on the head and for which the head contact point on the vehicle was known. For each case there was also sufficient information available for a reasonable estimate to be made of the velocity of the head relative to the vehicle on impact. These cases were selected without reference to the nature and severity of any injury to the brain. Consequently, they include three cases in which no brain injury has been identified, death having been due to injury to another body region.

HEAD IMPACT CALCULATIONS

Despite several years of application of both the two dimensional and three dimensional versions of the MADYMO mathematical model to the reconstruction of pedestrian/vehicle collisions we have not been able to achieve adequately reliable estimates of head impact velocity. This was because the kinematics of the articulated rigid body model used in MADYMO differed from that of cadavers observed in laboratory tests and of living pedestrians, as inferred from the investigation of actual collisions. As stated in an earlier paper [14], the simulation has much stiffer legs than the human, which means that at impact the legs bounce off the front of the car and there is less penetration of the pelvis; also the torso of the MADYMO model does not conform to the front and top of the car as well as the human cadaver. These differences, together with lack of reliable data on key parameters, such as joint stiffness, lead to considerable uncertainties in the estimates of head impact velocity and hence acceleration.

We have developed a comparatively simple method of estimating the linear and angular accelerations of the head during impact with the surface of the car which uses data which was either readily available or which could be estimated directly. The equations used in these calculations are set out in Figure 2 and the derivations are shown in the Appendix. The basis of the calculations is summarized in the diagram in Figure 3.

It is assumed that at impact there is high instantaneous friction between the front of the car and the pelvis and that the spine acts as a mechanical link to accelerate the head down on to the bonnet of the car. The head impact velocity is assumed to be the same as the vehicle impact velocity for a collision with a flat-fronted van and approximately the same for conventional cars and other vehicles with a sloping front. The impact of the head on the vehicle is assumed to be normal to the surface of the skull and to the vehicle panel. It is also assumed that the head does not slide at impact. The marks observed at the head contact points on the vehicle suggest that this is a reasonable assumption.

The linear acceleration is calculated from the impact velocity, the mass of the head and an assumed combined stiffness for the skull, scalp, and panel which are treated as one. Estimates have been made for combinations of head and hard surfaces e.g. A-pillar, medium surfaces e.g. plenum, and soft surfaces e.g. bonnet. Rebound effects are ignored. The mass of the head is calculated from the total body mass of the pedestrian [15].

The angular acceleration is assumed to be due to the resultant force vector acting at a distance from the centre of gravity of the head and its magnitude is determined by the size of the offset, the moment of inertia of the head, and the maximum force developed during the impact. Offsets have been calculated for each combination of latitude and longitude of impact location on the head (Table 1). The moment of inertia of the head was estimated from Reference 13.

Validation of calculations

Data from a cadaver pedestrian car collision test carried out at Calspan was obtained from Dr. K. Digges of the US National Highway Traffic Safety Administration and was compared with the output from the above procedure. The appropriate variables were derived and entered into the above equations and also developed into an input data set for the MADYMO mathematical model. The values obtained by calculation, and by MADYMO simulation were compared with the accelerometer readings of the cadaver test.

The maximum linear acceleration measured for the cadaver was 216g, for the calculation 210g and for the MADYMO simulation, 290g.

The result of the calculations is similar to the cadaver value and shows that the force-penetration function of the calculations is reasonably close to reality, at least for this particular case. The value for MADYMO was high, as predicted by Gibson, Hinrichs and McLean. It was not possible to compare the calculations for angular accelerations, because this data was not available from the cadaver test.

BRAIN INJURY SEVERITY

The injuries which are evident on macroscopic and microscopic examination of each brain are recorded on line diagrams of the coronal cross sections at each of ten standard stations at 10mm intervals on the longitudinal axis of the brain. Each section is viewed from its occipital or rearward side. The evidence of injury is provided by vascular markers, e.g. haemorrhage, or the observation of blood cells outside of vessels; other evidence is tissue disruption, e.g. laceration. The injury within each sector of each cross section (Figure 1) is coded from 0 = no injury, 1 = small haemorrhages, 2 = confluent haemorrhage, e.g. whole width of cortex, through to 3 = loss of tissue. The cortex and white matter for each sector are coded separately. The presence of sub-dural or sub-arachnoid haemorrhage is also recorded.

The coded data for each brain are entered into a computer file. The distribution of injury for each sector and each cross-section of a brain can be displayed in a diagram in which the sectors and lobes of the cerebral hemispheres are opened out, rather like the segments of an orange, (e.g. Figure 1). The same computer file can be used to produce diagrams of the distribution of injury for a group of cases with impacts in a similar location. Another method of analysis is to use the sum of the injury severity in all sectors (the Brain Injury Density (BID)) for each case as a dependent variable in statistical analyses.

RESULTS

The characteristics of the 26 cases studied are summarised in Table 2. Ages ranged from 8 to 87 years; there were 8 females. The majority of the impacts occurred at velocities of from 50 to 65 km/h. The combined stiffness of the head and struck surface was rated as hard in 7 cases, medium in 10 and soft in 9 cases. The estimated linear acceleration ranged from 2,110 to 6,600 m/s^2, and the estimated angular acceleration from 6,840 to 50,370 rad/s^2. (It is emphasised that the values for linear and angular acceleration given below are estimates only). The brain injury density ranged from zero to 105. There were 9 lateral impacts i.e. within an arc of 60° centred on the 3 o'clock or 9 o'clock positions, and 8 occipital impacts, i.e. within an arc of 60° centred on the 6 o'clock position.

Severity of Impact and Injury

The relationship between brain injury density (BID) and severity of impact is shown separately for lateral and occipital impacts in Figures 4 and 5. In these diagrams BID is plotted against both angular acceleration and linear acceleration. For occipital impacts (Figure 4) linear acceleration ranged from just over 2,000 m/s^2 to about 6,500 m/s^2, while angular acceleration ranged from about 6,000 to 15,000 radians/ s^2. As the offset of the force vector from the centre of gravity of the head was small for these occipital impacts (given the assumptions made above) the acceleration of the head was primarily linear. For occipital impacts the BID generally increased with increasing acceleration, although at any particular acceleration level, the range of BID was quite large.

For lateral impacts there was no clear association between BID and acceleration (Figure 5). In these impacts there was a greater range of angular acceleration, from about 10,000 rad/s^2 to 50,000 rad/s^2, but a similar range of linear acceleration (2,000 to 6,600 m/s^2).

Distribution of Injury

We have examined the effects of increasing levels of acceleration on the distribution and severity of injury in the brain, for occipital and lateral impacts.

Occipital Impacts

The injury distributions for these impacts are presented in Figures 6 and 7 as though the impacts were all in the 165° zone, on the assumption that the head and brain are symmetrical about the longitudinal axis.

Figure 6 shows that for occipital impacts of less than 5,000 m/s^2 linear acceleration, injuries were concentrated in the frontal areas of the cerebral hemispheres, on the superior and inferior surfaces, and the temporal lobes. At higher linear acceleration levels (greater than 5,000 m/s^2) injuries were evenly spread over the inferior surface and concentrated over the occipital half of the superior surface (Figure 7). Both sides were equally affected, but with a suggestion that there was more injury on the superior surface of the impacted and on the inferior surface of the opposite side. Injury was observed in the central part of the central sector of the brain in both high and low acceleration groups.

Lateral Impacts

These cases were selected because the impacts fell within a 60° arc centred on the 3 o'clock or 9 o'clock position and on horizontal levels 1 and 2. The injury distributions for these cases are presented in Figures 8 and 9 as though the impacts were all on the right side of the head. This is done on the assumption that the head and brain are symmetrical about the longitudinal axis. At lower linear accelerations (Figure 8) injuries were more or less evenly spread on the inferior surface of the brain, but concentrated on the frontal area of the superior surface. The temporal lobe on the side of impact was more affected than that on the other side. For the impacts at the higher linear accelerations (greater than 5,000

m/s^2), the frontal area of the inferior surface suffered more injury, while injuries were more evenly distributed over the superior surface (Figure 9). The temporal lobe on the side of impact again suffered more injury. In the central sector, the frontal half was more affected in the higher severity impacts, with injuries being evenly spread in the less severe impacts.

DISCUSSION

The susceptibility of the frontal areas of the brain to injury in both occipital and lateral impacts of lower intensity, is demonstrated, as is the increasing involvement of the occipital regions, and the ipsi-lateral para-sagittal regions, in impacts of increasing severity. These findings are similar to those of Gennarelli et al. based on impacts to the heads of sub-human primates.[16]

These are preliminary results. They are based on a small number of cases and the accuracy of the acceleration estimates has yet to be proven. The main purpose of this paper has been to demonstrate the practicability of our method of studying brain injury mechanisms in actual crashes.

We believe that as further cases accumulate, and as we refine our methods of investigation and the detail of the model, the uncertainties will become less.

ACKNOWLEDGEMENTS

The authors wish to thank the State Coroner, Mr. K.B. Ahern for permission to attend autopsy examinations, and the staff of the Accident Investigation and Prevention Section, South Australian Police for their willing cooperation. We also wish to thank Dr. K. Digges of the US National Highway Traffic Safety Administration for his help in supplying the cadaver test data.

REFERENCES

1. Robertson JS, McLean AJ, Ryan GA. Traffic accidents in Adelaide, South Australia. Melbourne: Australian Road Research Board, 1966. (Special Report No. 1).

2. McLean AJ, Robinson GK. Adelaide in-depth accident study 1975-1979. Part 1: An overview. Adelaide: Road Accident Research Unit, University of Adelaide, 1979.

3. Ryan GA, Wright JN, Hinrichs RW, McLean AJ. An in-depth study of rural road crashes in South Australia. Canberra: Federal Office of Road Safety and Adelaide: Road Safety Division, 1988. (Report CR 78).

4. McLean AJ. Head first? The causes, consequences and relative importance of head injuries in urban crashes. In: Proceedings of American Association for Automotive Medicine Conference. Illinois: American Association for Automotive Medicine, 1981: 15-27.

5. McLean AJ. Adelaide in-depth accident study 1975-1979. Part 8: Summary and recommendations. Adelaide: Road Accident Research Unit, University of Adelaide, 1981.

6. Cooter RD, David, DJ, McLean AJ, Simpson DA. Motorcyclist helmet-induced fatal skull base fracture. Lancet 1988; 1: 84-85.

7. Ommaya AK. Biomechanics of head injury: experimental aspects. In: Nahum AM, Melvin J, eds. The biomechanics of trauma. Connecticut: Appleton-Century-Crofts, 1985: 245-269.

8. Adams JH, Gennarelli TA, Graham DI. Brain damage in non-missile head injury: observations in man and sub-human primates. In: Smith WT, Cavanagh JB, eds. Recent advances in neuropathology. Edinburgh: Churchill Livingstone, 1982: 165-189.

9. Tarriere C. Relationship between experimental measuring techniques and real world injuries. In: Mackay M, Mellander H, Nilsson S, Petrucelli E, eds. Head injury mechanisms. Illinois: Association for the Advancement of Automotive Medicine, 1988: 797-803.

10. Garrott WR, Guenther D, Houk R, Lin J, Martin M. Improvement of methods for determining pre-crash parameters from skidmarks. Washington: National Highway Traffic Safety Administration, 1981. (Report DOT-HS-806-063).

11. Wood P. Impact and movement of pedestrians in frontal collisions with vehicles. Proceedings of Institution of Mechanical Engineers 1988; 202: 101-110.

12. Viano D, ed. Pedestrian impact injury and assessment. Warrendale: Society of Automotive Engineers, 1983. (Report P-121).

13. Melvin JW, Weber K, eds. Review of biomechanical impact response and injury in the automotive environment. Michigan: University of Michigan Transportation Research Institute, 1985; 11. (Report UMTRI-85-3).

14. Gibson TJ, Hinrichs RW, McLean AJ. Pedestrian head impacts: development and validation of a mathematical model. In: Proceedings of International IRCOBI Conference on the Biomechanics of Impacts. Bron: International Research Committee on Biokinetics of Impacts, 1986; 165-176.

15. Webb Associates, eds. Anthropometric source book. Volume 1: Anthropometry for designers. Washington: National Aeronautics and Space Administration, 1978; IV-34. (NASA Reference Publication 1024).

16. Gennarelli TA, Abel JM, Adams H, Graham D. Differential tolerance of frontal and temporal lobes to contusion induced by angular acceleration. In: Proceedings of Stapp Car Crash Conference. Warrendale: Society of Automotive Engineers, 1979: 561-586.

17. Macaulay MA. Introduction to impact engineering. London: Chapman & Hall, 1987.

18. Johnson W. Impact strength of materials. London: Edward Arnold, 1972.

Table 1

Offset of Force Vector From Centre of Gravity of Head* (millimetres)

Horizontal Angle (degrees)	Vertical Level on Head 0	1	2	3	4	5	6	7
15	10	10	20	10	20	50	70	50
45	10	20	30	20	10	40	60	40
75	0	20	40	30	10	30	40	30
105	0	30	40	30	20	30	40	30
135	0	20	30	30	20	20	60	70
165	0	10	10	20	20	10	70	110
195	0	10	10	20	20	10	70	110
225	0	20	30	30	20	20	60	70
255	0	30	40	30	20	30	40	30
285	0	20	40	30	10	30	40	30
315	10	20	30	20	10	40	60	40
345	10	10	20	10	20	50	70	50

* assumed Caucasian head shape

Table 2

Summary of Cases of Single Head Impacts

Case Number	Age (Years)	Sex	Site of Head Impact	Impact Velocity (km/h)	Impact Surface Stiffness	Linear Accel* (m/s^2)	Angular Accel* (rad/s^2)	Brain Injury Density
H005-84	74	Male	Lateral	45	Hard	4240	33160	13
H047-84	69	Male	Other	30	Medium	2190	11090	70
H018-85	55	Male	Other	65	Hard	6050	48460	15
H028-85	32	Male	Lateral	60	Hard	6230	40140	14
H050-85	62	Female	Lateral	60	Hard	6620	50370	53
H051-85	64	Male	Other	50	Medium	4080	16540	1
H070-85	14	Female	Lateral	50	Medium	4070	33200	51
H021-86	87	Male	Occipital	55	Soft	2700	6050	0
H029-86	39	Male	Occipital	60	Medium	4410	11020	40
H032-86	81	Male	Occipital	50	Soft	2380	5670	6
H047-86	68	Female	Other	50	Hard	5150	33690	36
H073-86	75	Female	Lateral	45	Soft	2260	9690	0
H078-86	21	Female	Occipital	55	Medium	4440	9200	3
H079-86	61	Male	Lateral	20	Hard	2110	8760	61
H012-87	20	Male	Occipital	85	Medium	6600	14780	57
H024-87	8	Male	Other	40	Medium	3730	11580	41
H037-87	64	Male	Lateral	55	Hard	5690	49230	32
H051-87	17	Female	Lateral	75	Soft	3620	16780	45
H053-87	54	Male	Other	60	Soft	2950	13200	2
H003-88	17	Female	Occipital	70	Medium	5590	11840	2
H006-88	16	Male	Other	50	Soft	2480	10890	56
H007-88	65	Male	Occipital	60	Soft	2840	6840	0
H011-88	30	Male	Occipital	80	Medium	6410	13480	105
H015-88	12	Male	Other	70	Soft	3910	13550	8
H020-88	75	Female	Lateral	80	Medium	5810	29750	90
H026-88	42	Male	Other	60	Soft	2940	13240	92

PEDESTRIAN BRAIN INJURY DENSITY
BY LINEAR AND ANGULAR ACCELERATION OF THE HEAD
8 OCCIPITAL HEAD IMPACTS

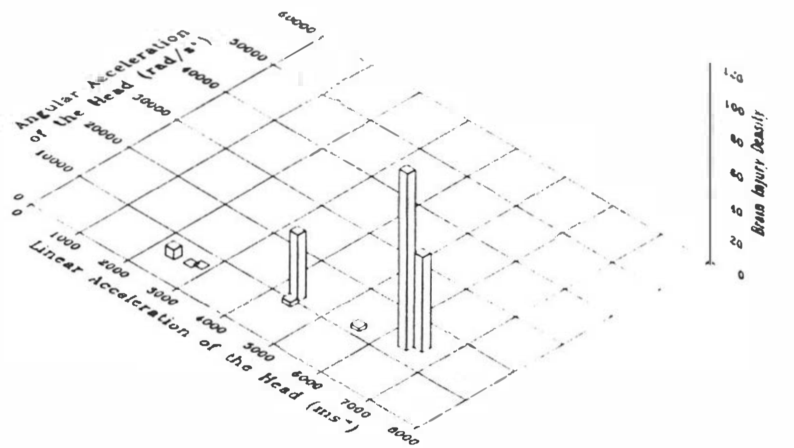

Figure 4

PEDESTRIAN BRAIN INJURY DENSITY
BY LINEAR AND ANGULAR ACCELERATION OF THE HEAD
9 RIGHT LATERAL HEAD IMPACTS

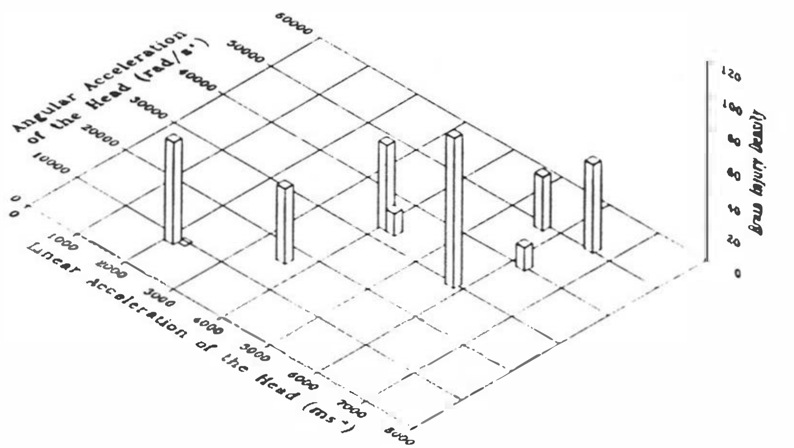

Figure 5

APPENDIX

DERIVATION OF EQUATIONS FOR LINEAR AND ANGULAR ACCELERATION [Refs 17,18]

During the loading phase of the impact of a head normal to the surface of an object (such as the bonnet of a car) we assume that there is complete transformation of kinetic energy to strain energy, assuming that the impacted object itself is not accelerated.

That is: $$1/2Mv^2 = 1/2Fd \quad [1]$$

where M = mass of head (kg)

v = velocity of head relative to the impacted object (m/s)

F = force acting on the head due to the impact (N)

d = combined deflection of head and impacted object (m).

If K (N/m) is the combined stiffness of the head and the struck object, and it is assumed that this stiffness is constant, then equation [1] can be expressed as:

$$1/2\ Mv^2 = Kd^2 \quad [2]$$

or $$d = v\ (M/K) \quad [3].$$

From force balance considerations,

$$Ma = Kd \quad [4]$$

where a = the linear acceleration of the centre of gravity of the head (m/s^2)

from equations [3] and [4] we get:

$$a = v\ (K/M) \quad [5].$$

The angular acceleration (radians/sec^2) is:

$$= F.x/I \quad [6]$$

where x (m) is the offset of the force vector from the centre of gravity of the head and I ($kg.m^2$) is the moment of inertia of the head.

BRAIN INJURY DISTRIBUTION (CUMULATIVE SEVERITY)
5 OCCIPITAL IMPACTS WITH LINEAR ACCELERATION < 5000 ms^{-2}

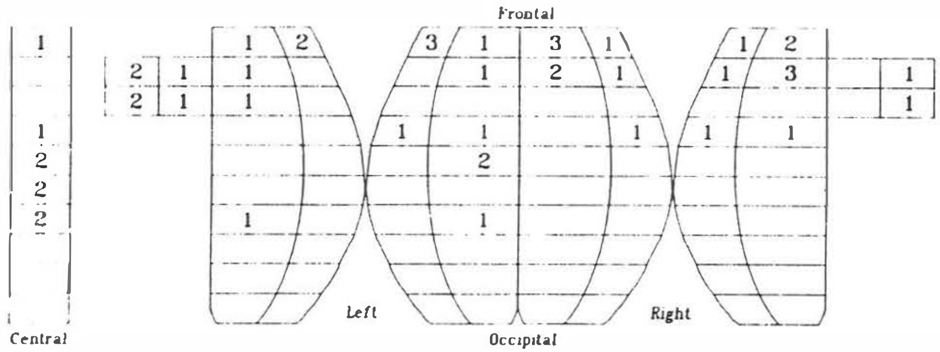

FIGURE 6

BRAIN INJURY DISTRIBUTION (CUMULATIVE SEVERITY)
3 OCCIPITAL IMPACTS WITH LINEAR ACCELERATION > 5000 ms^{-2}

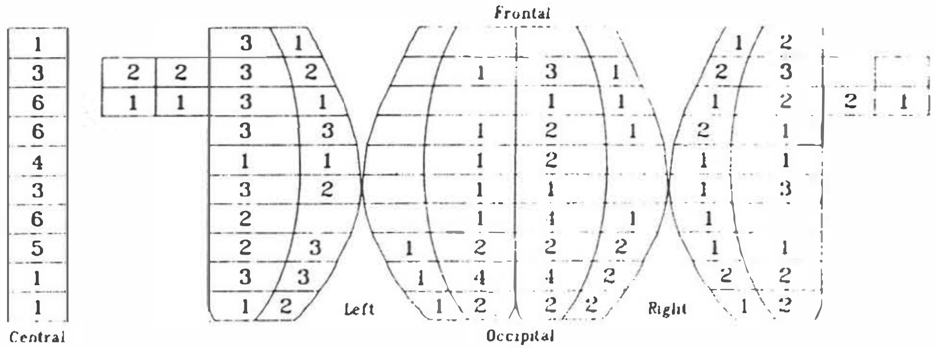

FIGURE 7

BRAIN INJURY DISTRIBUTION (CUMULATIVE SEVERITY)
5 LATERAL IMPACTS WITH LINEAR ACCELERATION < 5000 ms^{-2}

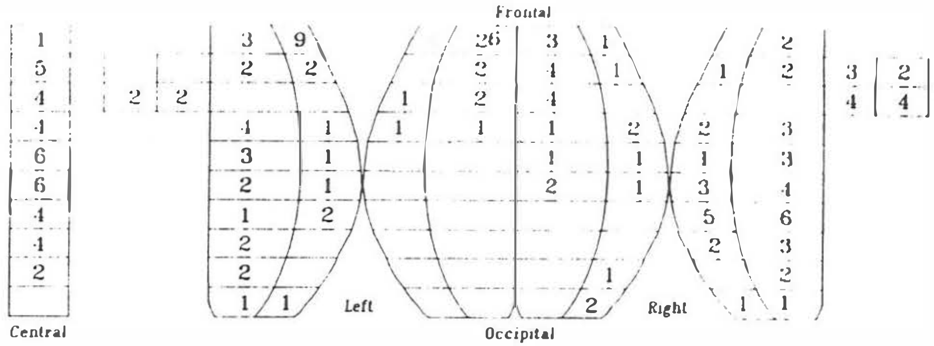

FIGURE 8

BRAIN INJURY DISTRIBUTION (CUMULATIVE SEVERITY)
4 LATERAL IMPACTS WITH LINEAR ACCELERATION > 5000 ms^{-2}

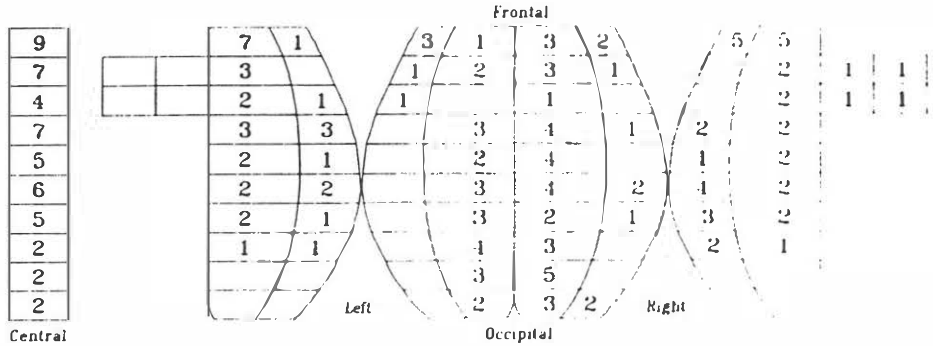

FIGURE 9

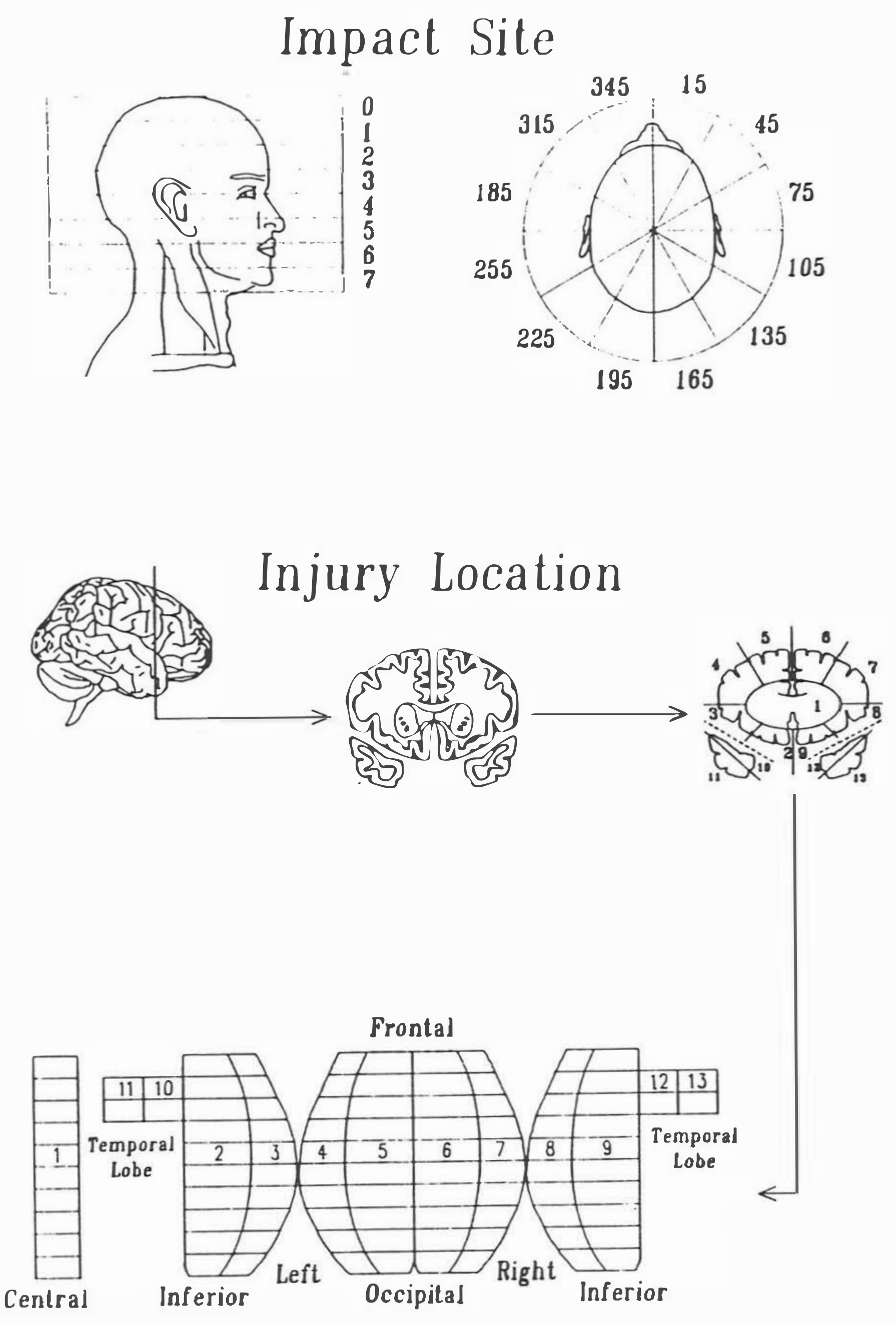

FIGURE 1

SUMMARY OF HEAD IMPACT CALCULATIONS

(1) $a = v\sqrt{(K/M)}$ m/s^2

(2) $F = M a$ N

(3) $\alpha = (F \cdot x)/I$ rad/s^2

(a) $M = 0.0306(T) + 2.46$ kg

(b) $I = 0.02$ $kg\ m^2$

(c) $K = 600{,}000$ N/m (hard surface)

$= 350{,}000$ N/m (medium surface)

$= 140{,}000$ N/m (soft surface)

v - Velocity of the head at impact

a - Linear acceleration of the head due to impact

F - Force on the head due to impact

α - Angular acceleration of the head due to impact

K - Combined stiffness of the head and vehicle

M - Mass of the head

x - Offset of force vector from head center of gravity

I - Moment of inertia of the head

T - Total body mass of the pedestrian

FIGURE 2

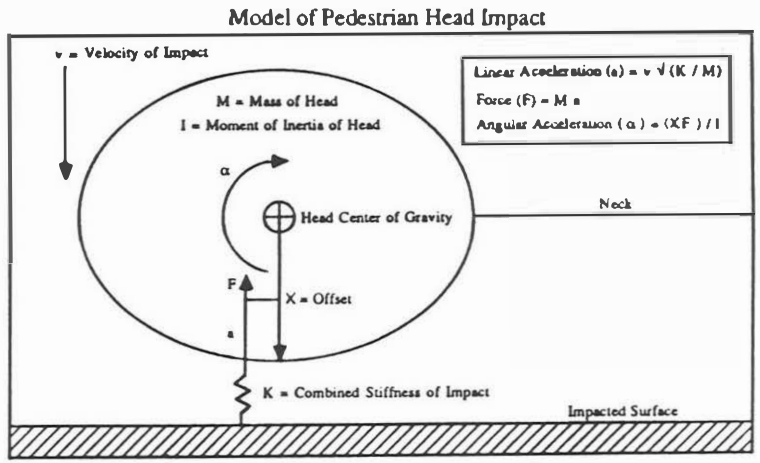

Figure 3